

# Non-Resonant Probing of the Methyl Fragment at 213 nm following 266nm Photolysis of Methyl Iodide

Monali Kawade,<sup>†</sup> Sumitra Singh,<sup>†</sup> and G. Naresh Patwari

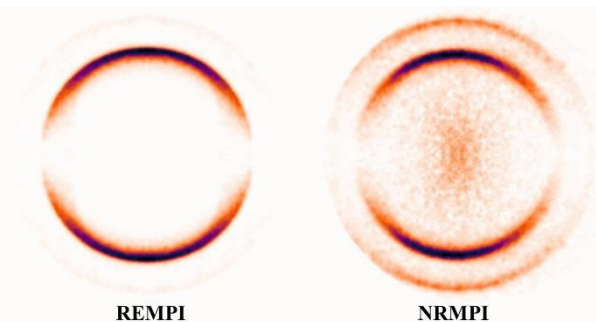
Department of Chemistry, Indian Institute of Technology Bombay, Powai, Mumbai  
400076 INDIA

\*E-mail: naresh@chem.iitb.ac.in

<sup>†</sup> These authors have contributed equally

## ABSTRACT

The velocity map imaging of the methyl radical formed by 266 nm photolysis of methyl iodide using 213 nm non-resonant multi-photon ionization (NRMPI) method. Comparison of the NRMPI method with the well-known (2+1) resonance multi-photon ionization (REMPI) method at 333.45 nm, which selectively probes Q-branch of band-origin transition of the methyl radical, indicates that the NRMPI method yields a significantly higher I/I\* branching ratio in comparison to the REMPI method, even though the velocity map images of both the methods are qualitatively similar. The higher I/I\* branching ratio obtained in the NRMPI method is attributed to the non-



resonant ionization of higher quanta states of the umbrella bending mode along with higher rotational states of the methyl fragment in the CH<sub>3</sub>+I dissociation channel. Thus, results obtained in the present work signify that a 213 nm excitation source, which is easily available as the fifth harmonic of Nd:YAG laser, can be used as an alternative and efficient probe to investigate photodissociation dynamics of polyatomic molecules.

## INTRODUCTION

The fundamental understanding of molecular dynamics, such as energy transfer processes in molecular reactions and photodissociation events can be achieved only if the internal energies and velocities of all products are specified. The specific information about the velocities of various molecular fragments forming in a bond-dissociation event requires simultaneous measurement of the speed of the particles and their angular distribution. Velocity map imaging is an extensively used to that approaches the goal of determining the three-dimensional velocity distribution of the state-selected product following a particular bond-dissociation event.<sup>1-5</sup> Velocity-map imaging in combination with laser pump-probe methods has been the experimental technique of choice for study gas-phase molecular photodissociation processes.<sup>6,7</sup> In the pump-probe method, photofragments formed in a photodissociation event by pump laser can be selectively probed to obtain highly resolved translational energy distributions of state selected states by resonance-enhanced multiphoton ionization (REMPI) method.<sup>8</sup> However, state selective probing of the molecular fragments by REMPI would require tuning of probe laser to the appropriate wavelength according to the energies of different states. In the case of larger molecules, resulting in multiple fragments after dissociation, state-selective study via REMPI becomes cumbersome and time-consuming. In such a scenario, non-resonance multi-photon ionization (NRMPI) method can be explored to probe the photofragments in a wide-range of quantum states.

Photodissociation dynamics of methyl iodide ( $\text{CH}_3\text{I}$ ) have been extensively explored for more than two decades which makes this system a benchmark for testing the abilities of newer methods in the photo-fragment imaging field.<sup>2,7-15</sup> Most of the studies on the methyl iodide photodissociation are focused on near UV excitation of the molecule to A-band, a broad absorption band in the 220-350nm range with an absorption maximum around 260 nm.<sup>7,9,10,16</sup> In general, excitation to the A-band of methyl iodide results in the dissociation of the C-I bond, which produces spin-orbit excited and ground state iodine along with methyl radical primarily in the ground electronic state. The methyl radical produced in the ground state can be selectively probed using the Q-branch of band-origin transition by 2+1 REMPI method using 333.45 nm laser.<sup>8</sup> On the other hand, the NRMPI method using wavelengths in the 325-335 nm region (very close to 2+1 REMPI

wavelength of 333.5 nm)<sup>16</sup> and 800nm femtosecond pump-probe scheme<sup>10</sup> have been reported. Additionally, universal detection via single-photon ionization by 118 nm VUV radiation has also been reported.<sup>17</sup> In this work, we are revisiting the well-studied dissociation dynamics of methyl iodide following 266 nm excitation using a conveniently available 213 nm (fifth harmonic of a Nd:YAG laser) as a NRMPI probe to investigate dynamics of methyl radical formation and compare with the well-known 333.45 nm 2+1 REMPI scheme. Further, investigation on 213 nm photolysis followed by 333.45 nm 2+1 REMPI detection of the methyl radical was also carried out as control experiments to ensure 213 nm radiation acts only as a NRMPI source.

## METHODOLOGY

The details of the velocity map imaging spectrometer are described elsewhere.<sup>18</sup> Briefly, helium gas at 3 atm pressure was passed over methyl iodide kept in a sample holder immersed in an ice bath and the resulting mixture expanded supersonically and skimmed to form a molecular beam. The molecular beam was intersected by counter-propagating pump (266 nm) and probe (333.45 nm for REMPI or 213nm for NRMPI) lasers. Cations produced were imaged using a four-electrode velocity map imaging (VMI) spectrometer fitted with a 50 mm diameter two-stage microchannel plate (MCP) and a P47 phosphor screen (MCP-50DLP47VF; Tectra). In the time-of-flight (TOF) mode, the front-plate of the MCP is grounded, the back-plate and the phosphor screen are held around +1500 V and a resistance-capacitor circuit (RC circuit) was used to extract the signal which is processed with a 350 MHz preamplifier (SR445A; Stanford Research Systems). In the imaging mode, the front-plate of the MCP detector is gated with a 75 ns pulse of -600 V (HTS 40-06-OT-75; Behlke), while the back-plate and the phosphor are held at +1200 and +3000 V, respectively. The gate time of the front plate is adjusted to match the arrival time of the desired ion. The image on the phosphor screen was recorded with a high-performance, easy-to-use USB, GigE CMOS camera (IDS Imaging Development Systems), and the raw images were acquired using NuAcq software.<sup>5</sup> Acquired images were further processed (symmetrized) using ImageJ software,<sup>19</sup> and Abel inversion was carried out by the Basis Set Expansion method (BASEX) to extract the kinetic energy spectrum.<sup>16</sup> In the present set of experiments, 266 and 213 nm are the fourth and fifth harmonic of the Nd: YAG

lasers (Brilliant-B; Quantel and TRLiG 850-10; Litron, respectively) and the probe laser (333.45 nm) is a frequency-doubled output of a tunable dye laser (LiopStar-HQ; LIOP-TEK) pumped with the second harmonic of an Nd: YAG laser (Brilliant-B; Quantel). The plane of polarization of all the lasers is kept parallel to the plane of the detector. The delay between the pump and probe lasers is kept at approximately 10 ns. The timings of the opening of the pulsed nozzle, the two lasers (both flashlamp and Q-switch triggers), the front-plate gate of the MCP detector, and the opening of the camera shutter were electronically controlled with an 8-channel digital delay pulse generator (DDG-9520; Quantum Composers). The energy of the pump and probe lasers were kept around 1 mJ/pulse and 500  $\mu$ J/pulse, respectively. The laser flux was optimized such that methyl fragment intensity was negligible in the absence of probe laser.

## RESULTS and DISCUSSION

The photodissociation of methyl iodide following excitation to A-band, which is a broad continuum ranging from 220 nm to 350 nm with a maximum around 260 nm is well studied both theoretically<sup>20-23</sup> and experimentally.<sup>7,9,10,16,17</sup> The A-band of methyl iodide is a  $\sigma^* \leftarrow n$  excitation from the lone pair on iodine to the lowest anti-bonding molecular orbital resulting in three broad, optically allowed transitions to dissociative states namely  $^1Q_1$ ,  $^3Q_0$  and  $^3Q_1$ . The  $^3Q_0$  state with the major absorption between 240 to 280 nm leads to the formation of spin-orbit excited iodine I ( $^2P_{1/2}$ ), denoted as I\*, and a ground state methyl radical via parallel transition. In contrast, the  $^1Q_1$  and  $^3Q_1$  states contribute at the blue-edge and the red-edge of the band respectively, via weak perpendicular transitions leading to the formation of iodine in the spin-orbit ground state ( $^2I_{3/2}$ ), denoted as I, and methyl fragment in its electronic ground state. The methyl radical formed in the process can be selectively ionized via the 2+1 REMPI method using 333.45 nm laser and the angular distribution of velocity map images corresponding to parallel and perpendicular transition can be characterized by angular anisotropy parameter of  $\beta = 2$  and  $-1$ , respectively.

The mass spectrum obtained following 266 nm pump and 333.45 nm probe experiment (Figure 1A) consists of an intense peak for methyl fragment ( $m/z=15$ ) along

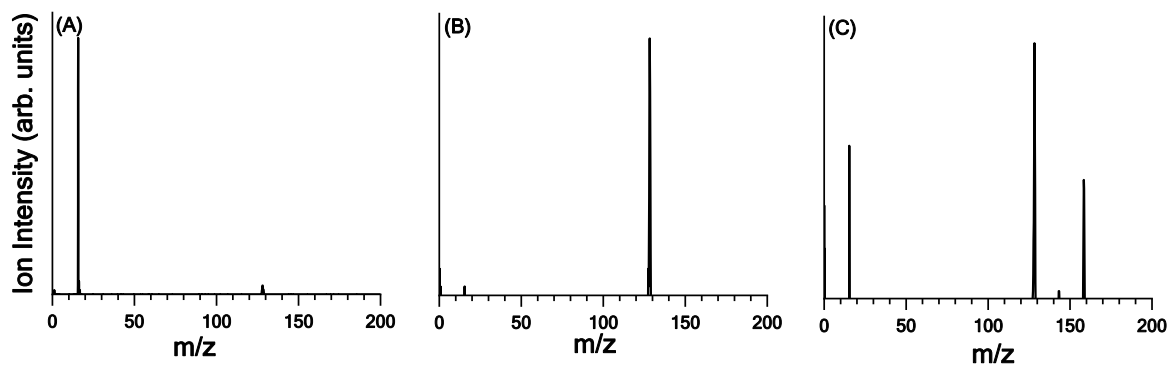


**Figure 1.** Mass spectra arising from (A) 266 nm pump and 333.45 nm probe, (B) 266 nm pump and 213 nm probe and (C) 213 nm pump and 333.45 nm probe. Pump only, probe only and background signals with pulse valve off condition were subtracted.

with a very low-intensity peak corresponding to the iodine atom ( $m/z=127$ ). On other hand, the mass spectrum obtained following the 266 nm pump and 213 nm probe experiment (Figure 1B) shows a very low-intensity peak for methyl fragment ( $m/z=15$ ) along with a strong peak corresponding to the iodine atom ( $m/z=127$ ). The relative intensities of the methyl fragment and iodine atom, in this case, suggests the non-resonant ionization of the methyl fragment by 213 nm probe laser. Further, the mass spectrum obtained following 213 nm pump and 333.45 nm probe experiment shows intense peaks for both methyl fragment and iodine atom accompanied by molecular ion peak ( $m/z=142$ ) and a peak corresponding to  $\text{CH}_3\text{I}\cdots\text{CH}_3$  complex ( $m/z=157$ ), which might occur due to photodissociation of methyl iodide molecular clusters.

The total translational energy ( $E_T$ ) profiles of the methyl fragments were extracted from the corresponding velocity map images recorded under various pump-probe conditions, which are shown in Figure 2. The velocity map image of the methyl radical obtained by 2+1 REMPI at 333.45 nm following 266 nm photolysis, depicted in Figure 2A, shows a bimodal distribution of velocities with maximum total translational energy ( $E_T^{\text{max}}$ ) values of 1.37 and 2.29 eV corresponding to the spin-orbital states  $\text{I}^*$  ( $^2\text{P}_{1/2}$ ) and  $\text{I}$  ( $^2\text{P}_{3/2}$ ), respectively, which are in good agreement with the experimental values reported earlier.<sup>17,24</sup> The images measured by 213 nm non-resonant multi-photon ionization (NRMPI) method following 266 nm photolysis, which can probe ground as well as vibrationally excited states of methyl fragment is shown in Figure 2B. In this case, the

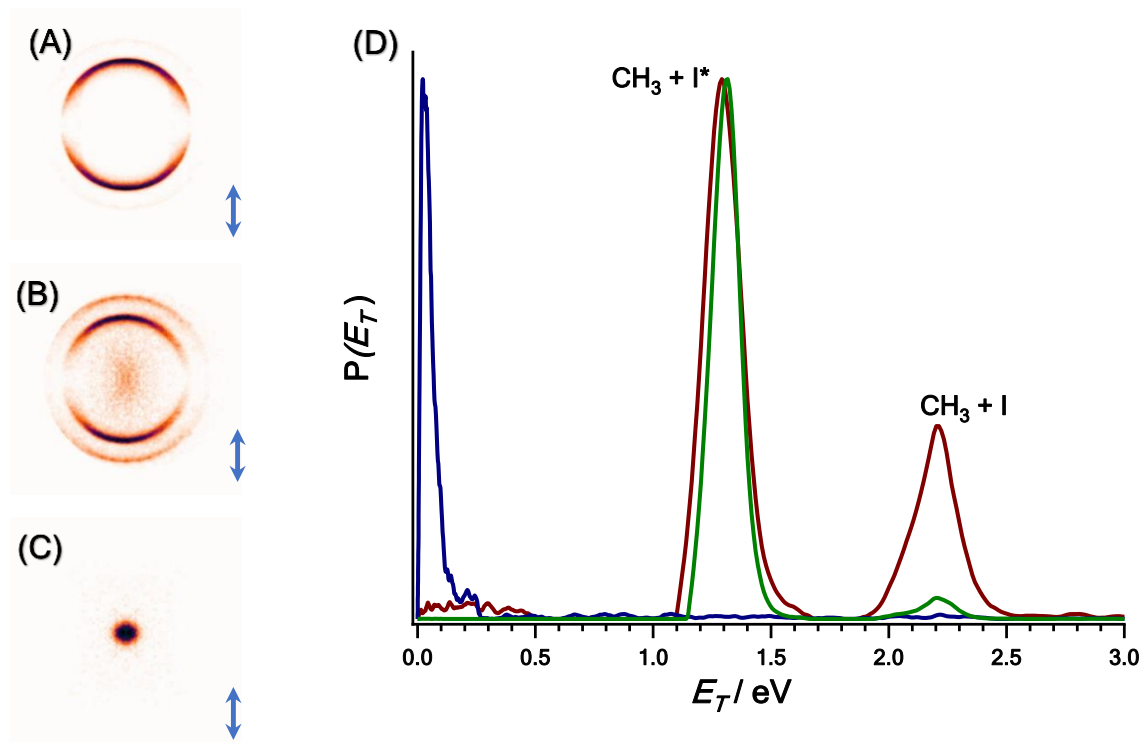


**Figure 2.** Velocity map images of the methyl fragment recorded by (A) 266 nm pump and 333.45 nm probe, (B) 266 nm pump and 213 nm probe, and (C) 213 nm pump and 333.45 nm probe. (D) The normalized total translational energy ( $E_T$ ) profiles for the images A, B, and C are shown in green, red and blue, respectively. All the images are shown on the same scale and the double-sided arrow indicates the laser polarization relative to the detector axis.

maximum total translational energy ( $E_T^{max}$ ) values are marginally higher for the  $I^*$  (1.39) and  $I$  (2.31 eV) in comparison with the 2+1 REMPI at 333.45 nm. Finally, the 213 nm photolysis followed by 2+1 REMPI of the methyl radical at 333.45 nm yields the image shown in Figure 2C. This image shows a bright central spot with very low total translational energy.<sup>14</sup> The total translational energy profiles, shown in Figure 2, indicate that the 2+1 REMPI (at 333.45 nm) and the NRMPI (at 213 nm) show similar features, however, the ratio of methyl radical yield in the  $I$  and  $I^*$  product channels ( $I/I^*$ ) is significantly higher for the NRMPI method (0.35) than the 2+1 REMPI method (0.06). It has been reported that the branching ratio of the methyl radical in the  $I/I^*$  product channel depends on the (2+1) REMPI probe wavelength in the 326-334 nm range, and has been attributed to population in 0 and 1 quanta of C–H stretching ( $\nu_1$ ) mode, 0, 1, and 2 quanta of umbrella bending ( $\nu_2$ ) mode and combinations thereof.<sup>7,8</sup> Further the  $CH_3+I$

dissociation channel is known to produce rotationally<sup>25</sup> and vibrationally<sup>7,8,24</sup> excited methyl radicals in comparison with the  $\text{CH}_3+\text{I}^*$  dissociation channel. Based on trajectory studies, abrupt change in geometry of methyl radical from pyramidal to planar takes place at the conical intersection of  $^3\text{Q}_0 - ^1\text{Q}_1$  state, which causes higher excitation of umbrella mode in  $\text{CH}_3+\text{I}$  channel. However, this geometry change is gradual in the case of  $\text{CH}_3+\text{I}^*$  channel resulting in much lower excitation of umbrella vibrational mode of methyl fragment produced in conjunction with  $\text{I}^*$ .<sup>20,21</sup> Therefore, the broadening of the kinetic energy distribution for the  $(\text{CH}_3+\text{I})$  product channel probed by 213 nm, in comparison to the 2+1 REMPI (at 333.45 nm) method, can be attributed to the additional contribution from the higher quanta of the umbrella bending ( $\nu_2$ ) mode along with the contribution from higher rotational states. The anisotropy parameter ( $\beta^*$ ) evaluated for the methyl radical produced in the  $\text{I}^*$  channels has a value very close to 2, which is in good agreement with the reported values and confirms the dominant contribution of parallel transition to  $^3\text{Q}_0$  state for  $\text{CH}_3+\text{I}^*$  channel. On the other hand, the anisotropy parameter ( $\beta$ ) evaluated for the methyl radical produced in the  $\text{I}$  channels has a value marginally lower than 2, which once again is in good agreement with earlier studies of 266nm photodissociation of methyl iodide and indicate some contribution of direct dissociation via a perpendicular transition to the  $^1\text{Q}_1$  or  $^3\text{Q}_1$  states.<sup>17</sup>

The total translational energy distribution profile for the methyl radical produced in the 213 nm pump and 333.45 nm probe experiment, also depicted in Figure 2D, shows near-zero kinetic energy distribution of the methyl fragments. Methyl iodide shows two prominent absorption bands in the range 220-350 nm (A-band; parallel) and 195-205 nm (B-band; perpendicular) with very low (almost nonexistent) absorption cross-section in the 205-200 nm range.<sup>14</sup> Thus, an almost negligible anisotropic character in the methyl images at 213nm photodissociation supports non-resonant electronic excitation of methyl iodide to some higher electronic state via multi-photon absorption resulting in almost zero available kinetic energy for the molecular fragments, in agreement with the observed experimental results.

## CONCLUSIONS

Photodissociation dynamics of methyl iodide via A-band excitation at 266nm, which is a benchmark for studying photodissociation dynamics of polyatomic molecules, is revisited in conjunction with NRMPI method using 213 nm laser. Comparison of the 213 nm NRMPI data with the results obtained from well-known (2+1) REMPI of methyl fragment indicates similar features in the velocity map images and the translational energy distribution profiled, with the exception of larger I/I\* branching ratio for the NRMPI method. The larger I/I\* branching ratio is attributed to the sampling of the higher quantum states of umbrella bending mode in CH<sub>3</sub>+I product channel with the NRMPI method. Further, photodissociation of methyl iodide at 213nm indicates only multi-photon excitation to some higher electronic state giving zero kinetic energy distribution of fragments, which ensures negligible contribution of 213 nm radiation to photolysis of methyl iodide in 266+213nm pump-probe scheme. Thus, the results discussed from photodissociation studies of a methyl iodide indicate NRMPI method using easily accessible 213nm (fifth harmonic of Nd: YAG laser) can be utilized as an effective alternative to REMPI detection of photodissociation products of polyatomic molecules in velocity map imaging measurements.

## ACKNOWLEDGMENTS

This study is based upon a work supported in part by the Science and Engineering Research Board of the Department of Science and Technology (Grant No. EMR/2016/000362) and Board of Research in Nuclear Sciences (BRNS Grant No. 58/14/18/2020) to GNP. SS thanks DST-INSPIRE for the research fellowship. MK is supported by the Women Scientists Scheme of the Department of Science and Technology (Grant No. SR/WOS-A/CS-18/2019). The authors wish to thank Ms. Namitha Brijit Bejoy and Mr. Prahlad Roy Chowdhury for their help with the experiments.

## REFERENCES

- (1) Whitaker, B. J Ed., *Imaging in Molecular Dynamics: Technology and Applications*; Cambridge University Press: Cambridge, 2003.



- (2) Chandler, D. W.; Houston, P. L. Two-Dimensional Imaging of State-Selected Photodissociation Products Detected by Multiphoton Ionization. *J. Chem. Phys.* **1987**, *87*, 1445–1447.
- (3) Eppink, A. T. J. B.; Parker, D. H. Velocity Map Imaging of Ions and Electrons Using Electrostatic Lenses: Application in Photoelectron and Photofragment Ion Imaging of Molecular Oxygen. *Rev. Sci. Instrum.* **1997**, *68*, 3477–3484.
- (4) Gebhardt, C. R.; Rakitzis, T. P.; Samartzis, P. C.; Ladopoulos, V.; Kitsopoulos, T. N. Slice Imaging: A New Approach to Ion Imaging and Velocity Mapping. *Rev. Sci. Instrum.* **2001**, *72*, 3848–3853.
- (5) Townsend, D.; Minitti, M. P.; Suits, A. G. Direct Current Slice Imaging. *Rev. Sci. Instrum.* **2003**, *74*, 2530–2539.
- (6) Techniques, I.; The, F. O. R.; Of, S.; Reaction, C. Study of Chemical Reaction Dynamics. *Annu. Rev. Phys. Chem.* **1995**, *46*, 335–372.
- (7) Eppink, A. T. J. B.; Parker, D. H. Energy Partitioning Following Photodissociation of Methyl Iodide in the A Band: A Velocity Mapping Study. *J. Chem. Phys.* **1999**, *110*, 832–844.
- (8) Chandler, D. W.; W. Thoman Jr., J.; Janssen, M. H. M.; Parker, D. H. Photofragment Imaging: The 266 Nm Photodissociation of CH<sub>3</sub>I. *Chem. Phys. Lett.* **1989**, *156*, 151–158.
- (9) De Nalda, R.; Durá, J.; García-Vela, A.; Izquierdo, J. G.; González-Vázquez, J.; Bañares, L. A Detailed Experimental and Theoretical Study of the Femtosecond A -Band Photodissociation of CH<sub>3</sub>I. *J. Chem. Phys.* **2009**, *128*, 244309.
- (10) Durá, J.; De Nalda, R.; Amaral, G. A.; Bañares, L. Imaging Transient Species in the Femtosecond A -Band Photodissociation of CH<sub>3</sub>I. *J. Chem. Phys.* **2009**, *131*, 134311.
- (11) Howard Failbrother, D.; Briggman, K. A.; Weitz, E.; Stair, P. C. Ultraviolet Photodissociation Dynamics of Methyl Iodide at 333 nm. *J. Chem. Phys.* **1994**, *101*, 3787–3791.
- (12) Xu, H.; Pratt, S. T. Photodissociation of Methyl Iodide via Selected Vibrational Levels of the B~ (2E<sub>3/2</sub>)6s Rydberg State. *J. Phys. Chem. A* **2015**, *119*, 7548–7558.
- (13) Marggi Poullain, S.; González, M. G.; Samartzis, P. C.; Kitsopoulos, T. N.; Rubio-Lago, L.; Bañares, L. New Insights into the Photodissociation of Methyl Iodide at 193 Nm: Stereodynamics and Product Branching Ratios. *Phys. Chem. Chem. Phys.* **2015**, *17*, 29958–29968.
- (14) González, M. G.; Rodríguez, J. D.; Rubio-Lago, L.; Bañares, L. Imaging the Stereodynamics of Methyl Iodide Photodissociation in the Second Absorption Band: Fragment Polarization and the Interplay between Direct and Predissociation. *Phys. Chem. Chem. Phys.* **2014**, *16*, 26330–26341.
- (15) Baronavski, A. P.; Owrutsky, J. C. Vibronic Dependence of the Ë State Lifetimes of CH<sub>3</sub>I and CD<sub>3</sub>I Using Femtosecond Photoionization Spectroscopy. *J. Chem. Phys.* **1998**, *108*, 3445–3452.
- (16) Poullain, S. M.; Chicharro, D. V.; Rubio-Lago, L.; García-Vela, A.; Bañares, L. A Velocity-Map Imaging Study of Methyl Non-Resonant Multiphoton Ionization from the Photodissociation of CH<sub>3</sub>I in the A-Band. *Philos. Trans. R. Soc. A Math. Phys. Eng.*

*Sci.* **2017**, 375, 20160205.

- (17) Gardiner, S. H.; Lipciuc, M. L.; Karsili, T. N. V.; Ashfold, M. N. R.; Vallance, C. Dynamics of the A-Band Ultraviolet Photodissociation of Methyl Iodide and Ethyl Iodide via Velocity-Map Imaging with “universal” Detection. *Phys. Chem. Chem. Phys.* **2015**, 17, 4096–4106.
- (18) Mishra, S.; Bejoy, N. B.; Kawade, M.; Upadhyaya, H. P.; Patwari, G. N. Photodissociation of O-Xylene at 266 Nm: Imaging the CH<sub>3</sub> Dissociation Channel. *J. Chem. Sci.* **2021**, 133, 128.
- (19) Schneider, C. A.; Rasband, W. S.; Eliceiri, K. W. NIH Image to ImageJ: 25 Years of Image Analysis. *Nat. Methods* **2012**, 9, 671–675.
- (20) Amatatsu, Y.; Morokuma, K.; Yabushita, S. Ab Initio Potential Energy Surfaces and Trajectory Studies of A-Band Photodissociation Dynamics: CH<sub>3</sub>I\*→CH<sub>3</sub> + I and CH<sub>3</sub> + I\*. *J. Chem. Phys.* **1991**, 94, 4858–4876.
- (21) Amatatsu, Y.; Yabushita, S.; Morokuma, K. Full Nine-Dimensional Ab Initio Potential Energy Surfaces and Trajectory Studies of A-Band Photodissociation Dynamics: CH<sub>3</sub>I\*→CH<sub>3</sub>+I, CH<sub>3</sub>+I\*, and CD<sub>3</sub>I\*→CD<sub>3</sub>+I, CD<sub>3</sub>+I\*. *J. Chem. Phys.* **1996**, 104, 9783–9794.
- (22) Arbelo-González, W.; Bonnet, L.; García-Vela, A. Semiclassical Wigner Theory of Photodissociation in Three Dimensions: Shedding Light on Its Basis. *J. Chem. Phys.* **2015**, 142, 134111.
- (23) Shapiro, M.; Bersohn, R. Vibrational Energy Distribution of the CH<sub>3</sub> Radical Photodissociated from CH<sub>3</sub>I. *J. Chem. Phys.* **1980**, 73, 3810–3817.
- (24) Eppink, A. T. J. B.; Parker, D. H. Methyl Iodide A-Band Decomposition Study by Photofragment Velocity Imaging. *J. Chem. Phys.* **1998**, 109, 4758–4767.
- (25) Ogorzalek Loo, R.; Haerri, H. P.; Hall, G. E.; Houston, P. L. Methyl Rotation, Vibration, and Alignment from a Multiphoton Ionization Study of the 266 nm Photodissociation of Methyl Iodide. *J. Chem. Phys.* **1989**, 90, 4222–4236.